Jordanian Journal of Computers and Information Technology (JJCIT), Vol. 12, No. 02, June 2026.

ON THE EFFECT OF KEYHOLE CHANNEL IN RSMA NETWORKS: A THEORETICAL OUTAGE ANALYSIS

Hong-Nhu Nguyen[1] and Phong-Cuong Ngo[2]

(Received: 20-Feb.-2026, Revised: 16-Apr.-2026, Accepted: 30-Apr.-2026)

ABSTRACT

This paper examines the theoretical performance of rate-splitting multiple access (RSMA) in keyhole fading channels. This rank-deficient environment is notorious for degrading the performance of traditional single-input single-output (SISO) systems. For a two-user downlink channel, exact and asymptotic outage probability results of RSMA with perfect and imperfect successive interference cancellation (pSIC and ipSIC) are derived. Closed-form solutions are derived by comparing the product of two independent Nakagami-m fading channels that model the keyhole effect. To further demonstrate RSMA's robustness in such an environment, we also examine the diversity order and unveil the effect of keyhole-induced rank deficiency on system reliability. Our results demonstrate that RSMA retains a performance edge over non-orthogonal multiple access (NOMA), especially with imperfect SIC or low SNR. Numerical results and Monte-Carlo simulations confirm the theoretical formulae and show that RSMA can combat the harmful effects of the keyhole channel better than other conventional schemes. The results confirm the promise of RSMA for future wireless systems operating in severe-fading environments.

KEYWORDS

Keyhole channel, Rate-splitting multiple access (RSMA), Outage probability, Nakagami-m, Imperfect SIC, Diversity order, Non-orthogonal multiple access (NOMA).

1. INTRODUCTION

Rate-Splitting Multiple Access (RSMA) has been an effective non-orthogonal transmission technique that is capable of bridging and surpassing traditional methods like Space-Division Multiple Access (SDMA) and Non-Orthogonal Multiple Access (NOMA) in a wide range of network scenarios. Through the splitting of user messages into common and private components, RSMA has more flexible interference management with partial decoding and interference treating, while enjoying better resilience to channel uncertainties and user deployments [1]-[3].

Although there have been comprehensive investigations considering RSMA under perfect propagation conditions, its performance in rank-deficient fading channels-more specifically, keyhole channels-has not received significant consideration. Such channels represent a particular form of spatial correlation in which the MIMO channel collapses to a rank-one variant of itself, significantly diminishing spatial multiplexing gains [4]-[6]. In realistic settings, like urban environments or tunnel passages, keyhole effects occur naturally as a result of physical limitations along signal-propagation paths.

In this paper, we investigate RSMA outage performance under keyhole fading. We consider a two-user downlink system and obtain exact and asymptotic results on the outage probability for pSIC and ipSIC. We also address the achievable diversity order and illustrate the effect of the keyhole on the reliability of the system. Our findings demonstrate that RSMA achieves a significant performance improvement over NOMA, especially when the SIC is imperfect or in the medium SNR range.

1.1 Related Work

RSMA has gained increasing attention for its potential to integrate and outperform classical multiple-access schemes in various performance aspects. Earlier works have investigated RSMA in the scenario of perfect MIMO channels, where ergodic capacity, energy efficiency and user fairness have been tackled [7]-[9]. More recently, analytic works have started investigating the outage behavior of RSMA, particularly when the blocklength is finite and there are short-packet constraints [10]-[13].

Keyhole fading, on the other hand, has been a well-known severe limitation to MIMO systems, which

1. H.-N. Nguyen is with Faculty of Technology and Engineering, Saigon Uni. (SGU), Ho Chi Minh City, Vietnam. Email: nhu.nh@sgu.edu.vn
2. P.-C. Ngo is with Faculty of Electrical and Electronics Eng., Ly Tu Trong College of Ho Chi Minh (LTTC), Chi Minh City, Vietnam. Email: ngophongcuong@lttc.edu.vn

has the tendency to make the spatial-diversity gain inoperative. Theoretical keyhole channel models are usually in the form of a product of two independent fading distributions and have been investigated under Nakagami- m, Rayleigh and Ricean conditions [14]-[17]. Recent advances have also significantly highlighted the necessity of analyzing multiple access and secure transmissions specifically over generalized Nakagami- m fading environments [18]-[19]. A number of works have obtained closed-form outage or bit error rate results in such channels, but primarily for single-user or conventional SISO setups.

To date, there have been limited attempts at marrying RSMA with keyhole channel modeling. Some initial attempts have looked at RSMA over correlated or rank-deficient channels, but typically resort to simulation-based analysis or approximations [20]-[21]. In this paper, we bridge the gap by presenting a systematic analytical treatment of RSMA over keyhole channels with exact expressions, asymptotic outage behavior and diversity order under both pSIC and ipSIC assumptions.

1.2 Motivation and Contributions

While RSMA continues to evolve as a powerful transmission technique, its performance under non-ideal propagation conditions is still a largely uncharted territory. Specifically, keyhole fading-where rich scattering does not provide spatial rank gain is a particular challenge for sophisticated multi-user communication strategies. Unlike conventional SISO fading, the keyhole channel model handles the extreme spatial correlation, which reduces the rank of the channel matrix to one, regardless of the number of antennas or spatial paths. Such a phenomenon can significantly reduce the spatial multiplexing gain that RSMA normally leverages to combat interference. Motivated by this limitation, we aim to theoretically characterize the behavior of RSMA under keyhole channels. Although a number of papers have dealt with outage performance of RSMA or keyhole channels separately, their intersection has never been exactly investigated. Also missing is the role of imperfect successive interference cancellation (ipSIC) under rank-deficient conditions. Not only of theoretical interest, but also of practical importance for system implementation in tunnels, indoor corridors or device-to-device environments with unfavorable scattering, it is to investigate the performance of RSMA under this adverse fading condition. The main contributions of this paper are as follows:

- Keyhole-aware outage analysis for RSMA: We present a new analytical method to analyze the outage probability of a two-user RSMA system in keyhole fading channels represented by the product of independent Nakagami-m distributions.
- Closed-form and asymptotic solutions: We obtain exact closed-form solutions for outage probability, followed by convenient asymptotic approximations at high SNR from which we can compute the diversity order analytically.
- Imperfect SIC included: Both perfect and imperfect SIC situations are taken into account within the analysis, so that realistic evaluation of the system performance under residual interference can be done.
- Comparison with NOMA: In order to provide a performance benchmark for RSMA, we also derive and simulate the outage performance of traditional NOMA in the same environment, showing the resilience of RSMA to keyhole-affected channels. All analytical results are confirmed by extensive Monte-Carlo simulations, proving the accuracy of the derived expressions and further illustrating the performance gain of RSMA over NOMA.

1.3 Organization

The rest of this paper is structured as follows: Section 2 presents the system model, such as the keyhole channel and RSMA scheme; Section 3 calculates the outage probability for pSIC and ipSIC cases; Section 4 investigates the diversity order; Section 5 provides numerical and simulation results comparing RSMA and NOMA; and Section 6 concludes the paper.

2. SYSTEM MODEL

2.1 System Architecture

We consider a downlink multi-user single-antenna RSMA system in which a base station (BS) communicates with N legitimate single-antenna users through a keyhole of scattering cross-section δ

that separates the BS and the users as shown in Fig. 1, where the BS-to-keyhole link g_0 and the keyhole-to-user n link g_n are each modeled as independent Nakagami- m fading processes, so that the overall channel gain to user n is the product $g_0 g_n$.

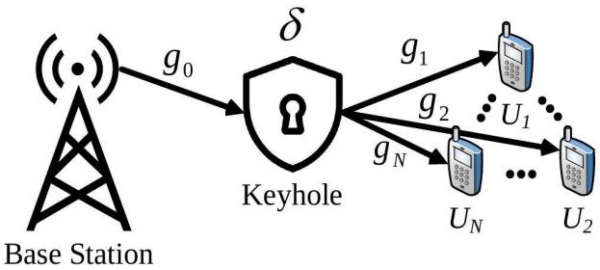

Figure 1. The system model of keyhole-based RSMA network.

2.2 Received Signals

To efficiently serve multiple users, the BS implements RSMA, which enables the simultaneous transmission of common and private messages. This strategy improves spectral efficiency and reduces inter-user interference. The transmitted signal is given by:

$$\bar{x} = \sqrt{P_S}\left(\sqrt{a_c}x_c + \sum_{n=1}^{N}\sqrt{a_n}x_n\right), \tag{1}$$

where P_S denotes the total transmitted power of the BS, x_c is the common message intended for all users with a power allocation coefficient a_c and x_n is the private message for the n^{th} user, assigned with power coefficient a_n, ensuring $a_c + \sum_{n=1}^{N} a_n = 1$.

The received signal at the n^{th} user, under the keyhole channel condition is given by:

$$\bar{y}_n = g_0\delta g_n\bar{x} + \omega_n = \underbrace{g_0\delta g_n\sqrt{a_c P_S}x_c}_{\text{Common message}} + \underbrace{g_0\delta g_n\sqrt{a_n P_S}x_n}_{\text{Desired private message}} + \underbrace{\sum_{j=1,j\neq n}^{N} g_0\delta g_n\sqrt{a_j P_S}x_j}_{\text{Interference}} + \underbrace{\omega_n}_{\text{AWGN}}, \tag{2}$$

where ω_n is the additive white Gaussian noise (AWGN) with variance N_0. To decode the intended message, each user employs SIC in a two-step decoding process:

2.2.1 Decoding the Common Message

User n first decodes the common message x_c, considering all private messages as interference. The corresponding Signal-to-Interference-plus-Noise Ratio (SINR) for decoding x_c at user n is given by:

$$\bar{\gamma}_{c,n} = \frac{a_c P_S\delta^2|g_0|^2|g_n|^2}{(1-a_c)P_S\delta^2|g_0|^2|g_n|^2 + N_0} = \frac{a_c\rho_S\delta^2|g_0|^2|g_n|^2}{(1-a_c)\rho_S\delta^2|g_0|^2|g_n|^2 + 1}. \tag{3}$$

where $\rho_S = P_S/N_0$ is the transmit signal-to-noise ratio (SNR). Note that x_c and x_n are supposed to be normalized unity power signals, i.e., $\mathbb{E}\{|x_c|^2\} = \mathbb{E}\{|x_n|^2\} = 1$ in which $\mathbb{E}\{.\}$ denotes expectation operation.

2.2.2 Decoding the Private Message

Once the common message x_c is successfully decoded and cancelled, each user proceeds to decode its respective private message x_n. The SINR expressions for the perfect and imperfect SIC (pSIC and ipSIC) cases are given by:

$$\bar{\gamma}_{p,n}^{\text{pSIC}} = \frac{a_n\rho_S\delta^2|g_0|^2|g_n|^2}{\rho_S\delta^2|g_0|^2|g_n|^2\sum_{j=1,j\neq n}^{N} a_j + 1} \tag{4a}$$

$$\bar{\gamma}_{p,n}^{\text{ipSIC}} = \frac{a_n\rho_S\delta^2|g_0|^2|g_n|^2}{\rho_S\delta^2|g_0|^2|g_n|^2\sum_{j=1,j\neq n}^{N} a_j + \varpi\rho_S|g_I|^2 + 1} \tag{4b}$$

Here, $\varpi = 0$ and $\varpi = 1$ correspond to the cases of pSIC and ipSIC, respectively. The residual interference caused by ipSIC is modeled using Rayleigh fading, where the corresponding complex

channel gain is represented as $g_I \sim \mathcal{CN}(0, \Omega_I)$, with $0 \leq \Omega_I < 1$ as suggested in [22]. In this context, $\mathcal{CN}(.,.)$denotes the complex Gaussian distribution.

2.3 Channel Distributions

When the wireless channel $g_b, b \in \{0, n\}$ follows a Nakagami- m distribution, the corresponding channel power gain $|g_b|^2$ follows a Gamma distribution. The probability density function (PDF) and cumulative distribution function (CDF) of this Gamma-distributed gain are provided below, under the assumption that the fading parameter m_b is an integer greater than or equal to one [23]-[24].

$$f_{|g_b|^2}(x) = \frac{x^{m_b-1}}{\Gamma(m_b)\Omega_b^{m_b}} e^{-\frac{x}{\Omega_b}} \tag{5}$$

$$F_{|g_b|^2}(x) = 1 - \frac{1}{\Gamma(m_b)}\Gamma\left(m_b, \Omega_b^{-1}x\right) = 1 - e^{-\frac{x}{\Omega_b}} \sum_{p=0}^{m_b-1} \frac{x^p}{p!\,\Omega_b^p}, \tag{6}$$

where $\Omega_b \triangleq \lambda_b/m_b$ in which λ_b and m_b representing the mean and integer fading factor, respectively.

$\Gamma(.,.) and \Gamma(.)$ stands for the upper incomplete Gamma function and the Gamma function, respectively. It is worth noting that the second line of Eq. (6) holds only when m_b is an integer.

Remark 1: It is worth mentioning that although the Nakagami fading parameter m can generally assume any real value $m \geq 0.5$, we constrain m_b to be an integer in our derivations. This mathematical assumption is widely adopted in the literature to express the incomplete Gamma function as a finite series, which is a pivotal step to obtain closed-form mathematical expressions. The general performance trends and insights drawn from this integer assumption remain fully applicable to scenarios with non-integer fading parameters.

On the other hand, the PDF and CDF of the product of two squared Nakagami-m random variables, $\mathcal{G}_b \triangleq |g_0|^2|g_n|^2$, is given as follows [25]:

$$f_{\mathcal{G}_b}(x) = \frac{2x^{\frac{m_0+m_n}{2}} - 1}{\Gamma(m_0)\Gamma(m_n)(\Omega_0\Omega_n)^{\frac{m_0+m_n}{2}}} K_{m_0-m_n}\left(\sqrt{\frac{4x}{\Omega_0\Omega_n}}\right), \tag{7}$$

$$F_{\mathcal{G}_b}(x) = 1 - \sum_{p=0}^{m_0-1} \frac{2}{p!\,\Gamma(m_n)}\left(\frac{x}{\Omega_0\Omega_n}\right)^{\frac{p+m_n}{2}} K_{m_n-p}\left(\sqrt{\frac{4x}{\Omega_0\Omega_n}}\right), \tag{8}$$

Here, $K_q(.)$ is the modified Bessel function of the second kind [[26], Eq. (8.407)] and $m_0 \in \mathbb{N}$ denotes a positive integer fading parameter.

Additionally, Rayleigh-distributed RVs of $|g_I|^2$ have exponential distributions with $f_{|g_I|^2}(x) = \frac{1}{\Omega_I} e^{-\frac{x}{\Omega_I}}$ and $F_{|g_I|^2}(x) = 1 - e^{-\frac{x}{\Omega_I}}$ in [27].

3. OUTAGE PROBABILITY

In RSMA-based transmission, each user receives a superposition of the common message, its own private message and the private messages intended for other users. The decoding process follows a two-step approach as described in (3), (4a) and (4b). If the SINRs for decoding the common and private messages fall below the respective thresholds $\gamma_{th}^{c,n}$ and $\gamma_{th}^{p,n}$, the link between the BS and the n^{th} user, affected by the keyhole channel condition, is considered to be in outage. In this context, $\gamma_{th}^{c,n} = 2^{R_{c,n}} - 1$ and $\gamma_{th}^{p,n} = 2^{R_{p,n}} - 1$ denote the corresponding SINR thresholds, while $R_{c,n}$ and $R_{p,n}$ represent the target rates for decoding the common and private messages, respectively.

3.1 Outage Probability with pSIC

Theorem 1. The outage probability of the BS-to- n^{th} user link under keyhole fading with pSIC is given by:

$$\mathcal{P}_{U_n}^{\text{pSIC}} = \begin{cases} 1 - \sum_{p=0}^{m_0-1} \frac{2}{p!\,\Gamma(m_n)} \left(\frac{\tilde{\gamma}_{th}^{p,n}}{\Omega_0\Omega_n}\right)^{\frac{p+m_n}{2}} K_{m_n-p}\left(\sqrt{\frac{4\tilde{\gamma}_{th}^{p,n}}{\Omega_0\Omega_n}}\right), & \text{if } \tilde{\gamma}_{th}^{c,n} \le \tilde{\gamma}_{th}^{p,n}, \\ 1 - \sum_{p=0}^{m_0-1} \frac{2}{p!\,\Gamma(m_n)} \left(\frac{\tilde{\gamma}_{th}^{c,n}}{\Omega_0\Omega_n}\right)^{\frac{p+m_n}{2}} K_{m_n-p}\left(\sqrt{\frac{4\tilde{\gamma}_{th}^{c,n}}{\Omega_0\Omega_n}}\right), & \text{if } \tilde{\gamma}_{th}^{c,n} > \tilde{\gamma}_{th}^{p,n}, \end{cases} \tag{9}$$

where $\tilde{\gamma}_{th}^{c,n} = \gamma_{th}^{c,n}/\delta^2\rho_S[a_c - (1-a_c)\gamma_{th}^{c,n}]$ and $\tilde{\gamma}_{th}^{p,n} = \gamma_{th}^{p,n}/\delta^2\rho_S[a_n - (1-a_c-a_n)\gamma_{th}^{p,n}]$. Moreover, the result in (9) is derived under the conditions $a_c > \gamma_{th}^{c,n}/(1+\gamma_{th}^{c,n})$ and $a_n > (1-a_c)\gamma_{th}^{p,n}/(1+\gamma_{th}^{p,n})$.

Proof. The outage probability at the n^{th} user with pSIC is given by:

$$\mathcal{P}_{U_n}^{\text{pSIC}} = \Pr(\bar{\gamma}_{c,n} < \gamma_{th}^{c,n} \cup \bar{\gamma}_{p,n}^{\text{pSIC}} < \gamma_{th}^{p,n}) = 1 - \Pr(\bar{\gamma}_{c,n} > \gamma_{th}^{c,n}, \bar{\gamma}_{p,n}^{\text{pSIC}} > \gamma_{th}^{p,n}). \tag{10}$$

Plugging $\bar{\gamma}_{c,n}$ and $\bar{\gamma}_{p,n}^{\text{pSIC}}$ from (3) and (4a) in (6), we have:

$$\mathcal{P}_{U_n}^{\text{pSIC}} = 1 - \Pr\left(\frac{a_c\rho_S\delta^2\mathcal{G}_b}{(1-a_c)\rho_S\delta^2\mathcal{G}_b + 1} > \gamma_{th}^{c,n}, \frac{a_n\rho_S\delta^2\mathcal{G}_b}{\rho_S\delta^2\mathcal{G}_b\sum_{j=1,j\neq n}^{N} a_j + 1} > \gamma_{th}^{p,n}\right). \tag{11}$$

After performing algebraic manipulations, Equation (11) can be rewritten as:

$$\mathcal{P}_{U_n}^{\text{pSIC}} = 1 - \Pr(\mathcal{G}_b > \tilde{\gamma}_{th}^{c,n}, \mathcal{G}_b > \tilde{\gamma}_{th}^{p,n}) = 1 - \Pr(\mathcal{G}_b > \hat{\gamma}_{th}) = F_{\mathcal{G}_b}(\hat{\gamma}_{th}), \tag{12}$$

where $\hat{\gamma}_{th} = \max(\tilde{\gamma}_{th}^{c,n}, \tilde{\gamma}_{th}^{p,n})$. Combining (8) into (12), (9) can be obtained and the proof is completed.

3.2 Outage Probability with ipSIC

From (3) and (4b), the outage probability with ipSIC can be calculated by:

$$\begin{aligned} \mathcal{P}_{U_n}^{\text{ipSIC}} &= \Pr(\bar{\gamma}_{c,n} < \gamma_{th}^{c,n} \cup \bar{\gamma}_{p,n}^{\text{pSIC}} < \gamma_{th}^{p,n}) = 1 - \Pr(\bar{\gamma}_{c,n} > \gamma_{th}^{c,n}, \bar{\gamma}_{p,n}^{\text{pSIC}} > \gamma_{th}^{p,n}) \\ &= 1 - \Pr\left(\frac{\frac{a_c\rho_S\delta^2\mathcal{G}_b}{(1-a_c)\rho_S\delta^2\mathcal{G}_b + 1} > \gamma_{th}^{c,n}}{\rho_S\delta^2\mathcal{G}_b\sum_{j=1,j\neq n}^{N} a_j + \varpi\rho_S|g_I|^2 + 1} > \gamma_{th}^{p,n}\right) \end{aligned} \tag{13}$$

Theorem 2. The outage probability of the BS-to- n^{th} user link under keyhole fading with ipSIC is expressed as:

$$\mathcal{P}_{U_n}^{\text{ipSIC}} \approx \left[1 - \sum_{p=0}^{m_0-1} \frac{2}{p!\Gamma(m_n)} \left(\frac{T_c}{\Omega_0\Omega_n}\right)^{\frac{p+m_n}{2}} K_{m_n-p}\left(\sqrt{\frac{4T_c}{\Omega_0\Omega_n}}\right)\right]\left(1 - e^{-\frac{x_0}{\Omega_I}}\right) + e^{\frac{1}{\varpi^\rho\Omega_I}}\left[e^{-\varphi_I T_c} - \right.$$

$$\left. \sum_{p=0}^{m_0-1}\sum_{q=1}^{Q} \frac{2\pi^2\varphi_I\sqrt{1-\xi_q^2}}{p!4Q\Gamma(m_n)} \left(\frac{1}{\Omega_0\Omega_n}\right)^{\frac{p+m_n}{2}} \sec^2\left(\frac{\pi(\xi_q+1)}{4}\right) \times \Delta(\xi_q)^{\frac{p+m_n}{2}} e^{-\varphi_I\Delta(\xi_q)} K_{m_n-p}\left(\sqrt{\frac{4\Delta(\xi_q)}{\Omega_0\Omega_n}}\right)\right] \tag{14}$$

where $T_c = \frac{\gamma_{c,th}}{\rho_S\delta^2[a_c-(1-a_c)\gamma_{c,th}]}$, $\varphi_I = \frac{1}{\varpi\rho_S\tilde{\gamma}_{th}^{p,n}\Omega_I}$, $\Delta(x) = \tan\left(\frac{\pi(x+1)}{4}\right) + T_c$, $\xi_q = \cos\left(\frac{2q-1}{2Q}\pi\right)$ and Q is a complexity-accuracy tradeoff parameter. In this paper, we verified through MATLAB simulations that setting $Q = 200$ is sufficient to achieve excellent convergence, providing a tight match between the exact integration and the analytical approximation.

Proof. The proof is provided in Appendix A.

3.3 Outage Probability for Baseline NOMA

For comparison, a conventional two-user NOMA scheme is considered where the base station superimposes the private messages directly without a common message ($a_c = 0$). Assuming User 1 and User 2 are the near and far users, respectively, the power allocation coefficients satisfy $a_1 < a_2$ with $a_1 + a_2 = 1$. The received SINR for User 2 to decode its own message is given by:

$$\gamma_2^{\text{NOMA}} = \frac{a_2\rho_S\delta^2\mathcal{G}_2}{a_1\rho_S\delta^2\mathcal{G}_2 + 1}. \tag{15}$$

User 1 performs SIC to decode User 2's message before decoding its own. The SINR for User 1 to decode User 2's message and its own message are, respectively, formulated as:

$$\gamma_{1\to 2}^{\text{NOMA}} = \frac{a_2\rho_S\delta^2\mathcal{G}_1}{a_1\rho_S\delta^2\mathcal{G}_1 + 1}, \gamma_1^{\text{NOMA}} = a_1\rho_S\delta^2\mathcal{G}_1. \tag{16}$$

Consequently, the exact outage probabilities for User 1 and User 2 under the keyhole environment can be explicitly derived as:

$$\mathcal{P}_{U_1}^{\text{NOMA}} = 1 - \Pr\left(\gamma_{1\to 2}^{\text{NOMA}} \geq \gamma_{th}^2, \gamma_1^{\text{NOMA}} \geq \gamma_{th}^1\right) = F_{\mathcal{G}_1}\left(\max(\tau_1, \tau_2)\right), \tag{17}$$

$$\mathcal{P}_{U_2}^{\text{NOMA}} = \Pr\left(\gamma_2^{\text{NOMA}} < \gamma_{th}^2\right) = F_{\mathcal{G}_2}(\tau_2), \tag{18}$$

where $\tau_2 = \frac{\gamma_{th}^2}{\rho_S\delta^2(a_2 - a_1\gamma_{th}^2)}$ under the condition $a_2 > a_1\gamma_{th}^2$ (otherwise $\mathcal{P}_{U_2}^{\text{NOMA}} = 1$), $\tau_1 = \frac{\gamma_{th}^1}{\rho_S\delta^2 a_1}, \gamma_{th}^n = 2^{R_{p,n}} - 1$ is the target threshold for User n and $F_{\mathcal{G}_b}(.)$ is the CDF of the product of two Nakagami-m random variables given in (8).

4. DIVERSITY ANALYSIS

To gain further insights, the diversity order reached by users in two situations can be determined in this section using the analytical data presented above. The diversity order is defined as [28], Eq. (18).

$$d_{\mathrm{U}_n}^{\star} = -\lim_{\rho_S\to\infty} \frac{\log\left(\mathcal{P}_{U_n}^{\infty,\star}(\rho_S)\right)}{\log\rho_S}, \star \in \{\text{pSIC, ipSIC}\}. \tag{19}$$

With the help of [29], the asymptotic expression for the outage probability at U_n under pSIC in the high-SNR regime ($\rho_S \to \infty$) can be formulated as:

$$\mathcal{P}_{\mathrm{U}_n}^{\infty,\text{pSIC}} \underset{\rho_S\to\infty}{\approx} \frac{\psi_n(4\hat{\gamma}_{th})^{m_0}}{2m_0(\Omega_0\Omega_n)^{m_0}}, \tag{20}$$

where the condition $|m_0 - m_n| = 0.5$ is mathematically adopted from [29] to facilitate the exact simplification of the associated mathematical functions (e.g., modified Bessel function) into an incomplete Gamma function. This specific half-integer difference is required to explicitly extract a tight asymptotic bound and determine the diversity order in the high-SNR regime and $\psi_n = \frac{2^{1-2m_0}\sqrt{\pi}}{\Gamma(m_0)\Gamma(m_n)}$. By substituting (20) into (19) and performing algebraic simplifications, the diversity order of U_n with pSIC is found to be equal to m_0. For ipSIC, when ρ_S goes to infinity, then we have $\bar{\gamma}_{c,n} \approx \frac{a_c}{1-a_c}$ and $\bar{\gamma}_{p,n}^{\text{ipSIC}} \approx \frac{a_n\delta^2|g_0|^2|g_n|^2}{\delta^2|g_0|^2|g_n|^2\sum_{j=1,j\neq n}^{N} a_j + \varpi|g_I|^2}$, the asymptotic expression for $\mathcal{P}_{\mathrm{U}_n}^{\infty,\text{ipSIC}}$ is calculated as:

$$\mathcal{P}_{\mathrm{U}_n}^{\infty,\text{ipSIC}} = \begin{cases} 1, & if\ \dfrac{a_c}{1-a_c} < \gamma_{th}^{c,n} \\ \Pr\left(\dfrac{a_n\delta^2|g_0|^2|g_n|^2}{\delta^2|g_0|^2|g_n|^2\sum_{j=1,j\neq n}^{N} a_j + \varpi|g_I|^2} < \gamma_{th}^{p,n}\right), & \text{otherwise} \end{cases} \tag{21}$$

It is noted that we can rewrite (21) as:

$$\mathcal{P}_{\mathrm{U}_n}^{\infty,\text{ipSIC}} = \Pr(\mathcal{G}_b < \phi_n|g_I|^2) = \frac{1}{\Omega_I}\int_0^{\infty} F_{\mathcal{G}_b}(\phi_n x)e^{-\frac{x}{\Omega_I}}dx \tag{22}$$

where $\phi_n = \frac{\gamma_{th}^{p,n}\varpi}{\delta^2\left(a_n - \gamma_{th}^{p,n}\sum_{j=1,j\neq n}^{N} a_j\right)}$. Now, invoking (8) into (22), we have $\mathcal{P}_{\mathrm{U}_n}^{\infty,\text{ipSIC}}$ is given by:

$$\begin{aligned}\mathcal{P}_{\mathrm{U}_n}^{\infty,\text{ipSIC}} &= \frac{1}{\Omega_I}\int_0^{\infty}\left[1 - \sum_{p=0}^{m_0-1}\frac{2}{p!\,\Gamma(m_n)}\left(\frac{\phi_n x}{\Omega_0\Omega_n}\right)^{\frac{p+m_n}{2}} K_{m_n-p}\left(\sqrt{\frac{4\phi_n x}{\Omega_0\Omega_n}}\right)\right]e^{-\frac{x}{\Omega_I}}dx \\ &= 1 - \sum_{p=0}^{m_0-1}\frac{2\phi_n^{\frac{p+m_n}{2}}}{p!\,\Gamma(m_n)\Omega_I(\Omega_0\Omega_n)^{\frac{p+m_n}{2}}}\int_0^{\infty} x^{\frac{p+m_n}{2}}e^{-\frac{x}{\Omega_I}}K_{m_n-p}\left(\sqrt{\frac{4\phi_n x}{\Omega_0\Omega_n}}\right)dx\end{aligned} \tag{23}$$

Exchanging the variable $t = \frac{4}{\pi}\arctan(x) - 1 \Rightarrow \tan\left(\frac{\pi(t+1)}{4}\right) = x \Rightarrow \frac{\pi}{4}\sec^2\left(\frac{\pi}{4}(t+1)\right)dt = dx$, we have $\mathcal{C}_1^{ipSIC}$ is given by:

$$\mathcal{P}_{\mathrm{U}_n}^{\infty,\mathrm{ipSIC}} = 1 - \sum_{p=0}^{m_0-1} \frac{\pi \phi_n^{\frac{p+m_n}{2}}}{p!\, 2\Gamma(m_n)\Omega_I(\Omega_0\Omega_n)^{\frac{p+m_n}{2}}} \int_0^{\infty} \sec\left(\frac{\pi(t+1)}{4}\right)\Theta(t)^{\frac{p+m_n}{2}} e^{-\frac{\Theta(t)}{\Omega_I}} \times K_{m_n-p}\left(\sqrt{\frac{4\phi_n\Theta(t)}{\Omega_0\Omega_n}}\right)dt$$

where $\Theta(t) = \tan\left(\frac{\pi(t+1)}{4}\right)$.

By applying the Gaussian-Chebyshev quadrature, (24) can be approximated as:

$$\mathcal{P}_{\mathrm{U}_n}^{\infty,\mathrm{ipSIC}} \approx 1 - \sum_{p=0}^{m_0-1} \frac{\pi^2 \phi_n^{\frac{p+m_n}{2}}}{p!2Q\Gamma(m_n)\Omega_I(\Omega_0\Omega_n)^{\frac{p+m_n}{2}}} \sum_{q=1}^{Q} \sqrt{1-\xi_q^2}\sec\left(\frac{\pi(\xi_q+1)}{4}\right) \times \Theta(\xi_q)^{\frac{p+m_n}{2}} e^{-\frac{\Theta(\xi_q)}{\Omega_I}} K_{m_n-p}\left(\sqrt{\frac{4\phi_n\Theta(\xi_q)}{\Omega_0\Omega_n}}\right) \quad (24)$$

By incorporating (24) into (19) and following a series of simplifications, it is possible to derive the diversity order of U_n in the context of ipSIC, which is determined to be 0, a finding that is further corroborated by the graphical representations presented in Section 6.

5. NUMERICAL RESULTS

In this Section, we present the simulated outcomes pertaining to the analyzed system and juxtapose them with analytical formulations to validate their accuracy. Absent any specific indications, we adopt the system parameters delineated below: $a_c = 0.4, R_{c,n} = 0.2, R_{p,1} = 0.2, R_{p,2} = 0.1$ and $\delta = 0.5$. Additionally, we examine a straightforward scenario with $N = 2$ with power distribution coefficients explicitly set as $a_1 = 0.24$ and $a_2 = 0.36$, ensuring the total power constraint $a_c + a_1 + a_2 = 1$ is strictly satisfied. For the channel gains, the mean values are set to $\lambda_0 = \lambda_1 = \lambda_2 = 1$. The selection of unity mean values corresponds to a normalized fading channel standard, which is widely adopted in the existing literature (e.g., [25],[28]) to evaluate baseline theoretical limits. This symmetric channel setup ensures that the performance comparison between RSMA and NOMA is evaluated under a generalized fading environment. The residual interference variance is set to $\Omega_I = 0.01$. Furthermore, the Gauss-Chebyshev parameter is chosen as $Q = 200$ to achieve a precise approximation [30].

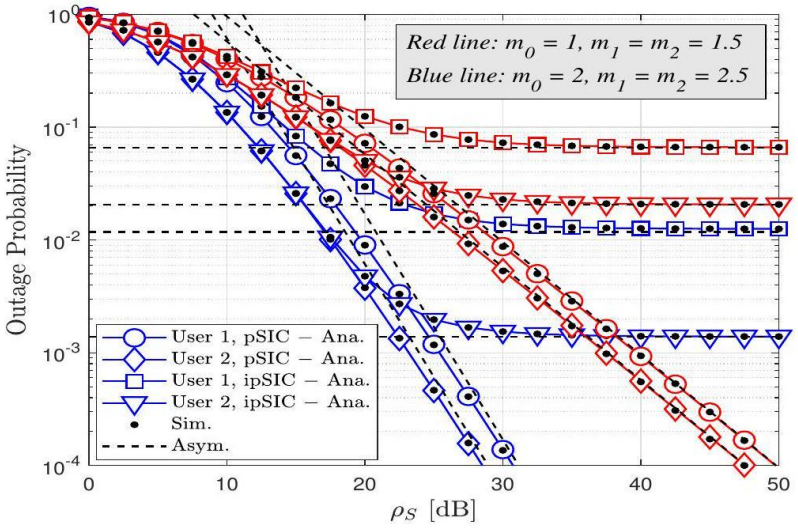

Figure 2. Outage performance *versus* ρ_S for $\mathrm{U_n}$.

Figure 2 shows the outage probability for two users under two sets of Nakagami-m parameters ($m_0 = 1, m_1 = m_2 = 1.5$ *vs.* $m_0 = 2, m_1 = m_2 = 2.5$) shows that increasing the fading severity parameters

consistently lowers the outage across all SNR values. At low SNR (10-20 dB), both curves drop sharply, indicating that even moderate increases in transmit power yield significant reliability gains despite the keyhole effect. In the high-SNR region (above 30 dB), both curves begin to flatten, reflecting the limited diversity imposed by the rank-one keyhole channel higher m values delay, but do not eliminate this outage floor.

Figure 3 depicts the comparison of RSMA and NOMA, RSMA maintains a clear outage advantage for both User 1 and User 2 across the entire SNR range, under both perfect and imperfect SIC assumptions. The performance gap widens in the mid-to-high SNR regime ($25-40$ dB), illustrating RSMA's superior interference mitigation under keyhole fading even a small amount of residual ipSIC interference hurts NOMA more severely.

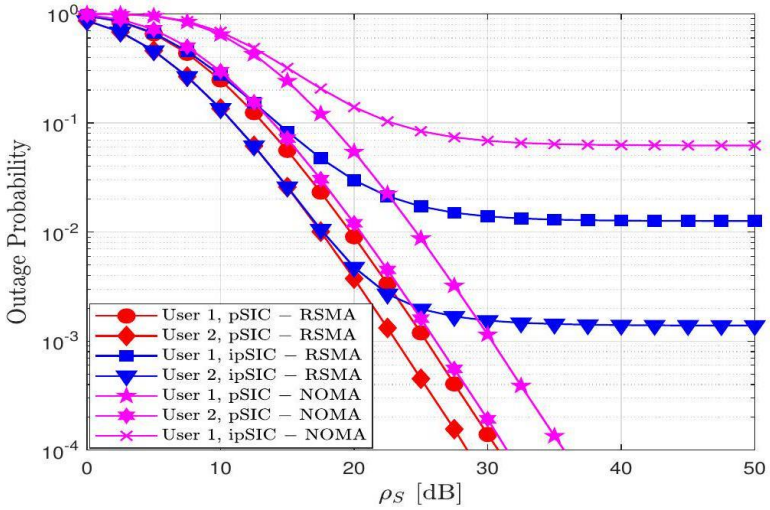

Figure 3. Comparison between RSMA and NOMA for the outage probability *versus* ρ_S.

Figure 4 shows outage probability against the common-message power coefficient a_c at two SNR values (20 dB dashed, 30 dB solid). It reveals an optimal allocation window around $a_c \approx 0.4 - 0.6$. Outside this window, the outage rises markedly: too little a_c starves the common stream and too much a_c reduces private-stream SINR. Increasing SNR shifts both curves downward, but preserves the same optimal region, confirming that power-split tuning remains critical under keyhole conditions.

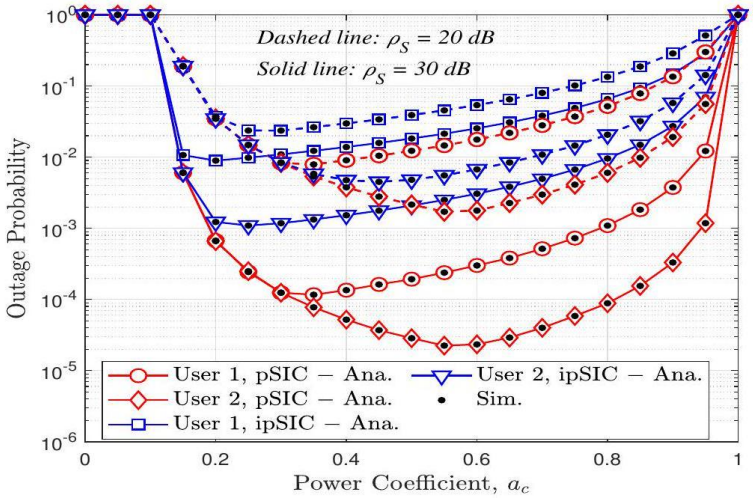

Figure 4. The outage probability versus power coefficient a_c with $m_0 = 2$ and $m_1 = m_2 = 2.5$.

Figure 5 depicts the outage probability *versus* the keyhole parameter δ at 30 dB. It displays a steep decline as δ increases (i.e., the keyhole attenuates less), demonstrating how stronger keyhole severity ($\delta < 0.2$) forces outage rates above 10^{-2}. For $\delta > 0.6$, the outage for higher Nakagami- m values ($m_0 = 3, m_1 = m_2 = 3.5$) plunges below 10^{-4}, indicating that RSMA benefits substantially from weaker keyhole effects and higher fading parameters. The gap between the two Nakagami- m curves also underscores how fading severity and keyhole strength jointly govern reliability.

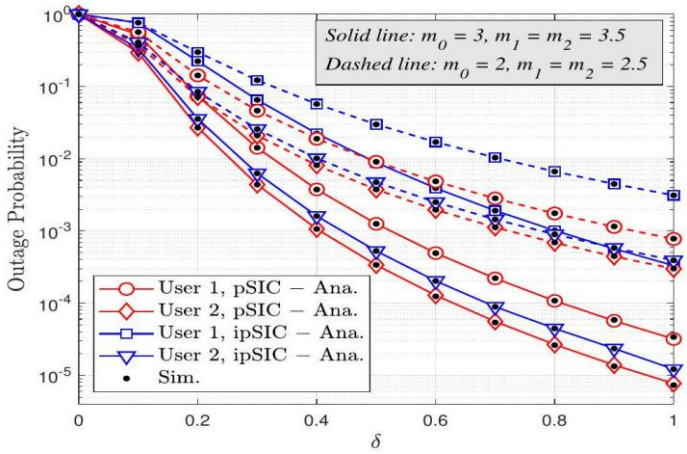

Figure 5. The outage probability *versus* the impact of the keyhole parameter δ with $\rho_S = 30$ dB.

6. CONCLUSIONS

This paper provides a unified analytical framework to assess the performance of RSMA in keyhole fading channels. Exact and asymptotic outage probabilities are established under perfect and imperfect SIC assumptions. The findings show that RSMA is more robust against the keyhole effect than traditional NOMA, especially in the presence of residual interference. Our analysis of diversity also shows that the keyhole channel degradation restricts the diversity attainable, but RSMA is resilient because of its adaptable message splitting framework. The expressions thus obtained agree well with simulation results and the theoretical analysis is therefore validated. The results offer a better understanding of RSMA performance under rank-deficient channels caused by spatial correlation or keyhole effects and support its applicability to practical wireless systems subject to spatial correlation.

Appendix A: Proof of Theorem 2

From (13), the outage probability occurs if either decoding step fails, i.e.

$$\mathcal{P}_{U_n}^{\text{ipSIC}} = 1 - \Pr\left(\mathcal{G}_b > \tilde{\gamma}_{th}^{c,n}, \mathcal{G}_b > \tilde{\gamma}_{th}^{p,n}(\varpi\rho_S|g_I|^2 + 1)\right) = 1 - \Pr\left(\mathcal{G}_b > \max\left(T_c, T_p(|g_I|^2)\right)\right), \quad (A.1)$$

Define thresholds

$$T_c \triangleq \tilde{\gamma}_{th}^{c,n} = \frac{\gamma_{c,th}}{\rho_S\delta^2\left[a_c - (1-a_c)\gamma_{c,th}\right]} \quad (A.2)$$

$$T_p(x) \triangleq \tilde{\gamma}_{th}^{p,n}(1+\varpi\rho_S x) = \frac{\gamma_{p,th}}{\rho_S\delta^2\left[a_n - \gamma_{p,th}\sum_{j\neq n} a_j\right]}(1+\varpi\rho_S x) \quad (A.3)$$

We have:

$$\max\left(T_c, T_p(x)\right) = \begin{cases} T_c, & T_p(x) \le T_c, \\ T_p(x), & T_p(x) > T_c. \end{cases} \quad (A.4)$$

Let $x = |g_I|^2$. By solving $T_p(x) = T_c$, we obtain:

$$T_p(x) \le T_c \Rightarrow x \le T_0 = \frac{T_c/T_p(0) - 1}{\varpi\rho_S} = \frac{\tilde{\gamma}_{th}^{c,n} - \tilde{\gamma}_{th}^{p,n}}{\varpi\rho_S\tilde{\gamma}_{th}^{p,n}}. \quad (A.5)$$

Then, outage probability becomes:

$$\mathcal{P}_{U_n}^{\text{ipSIC}} = \int_0^\infty F_{\mathcal{G}_b}\left(\max\left(T_c, T_p(x)\right)\right) f_{|g_I|^2}(x)dx = \underbrace{\frac{1}{\Omega_I}\int_0^{T_0} F_{\mathcal{G}_b}(T_c)e^{-\frac{x}{\Omega_I}}dx}_{I_1} + \underbrace{\frac{1}{\Omega_I}\int_{T_0}^\infty F_{\mathcal{G}_b}\left(T_p(x)\right)e^{-\frac{x}{\Omega_I}}dx}_{I_2} \quad (A.6)$$

where $f_x(x) = e^{-x/\Omega_I}/\Omega_I$ and $F_{\mathcal{G}_b}(\cdot)$ is the CDF of two squared Nakagami- m RVs. From (8), we have I_1 is calculated as:

$$I_1 = F_{\mathcal{G}_b}(T_c)\left(1 - e^{-\frac{x_0}{\Omega_I}}\right) = \left[1 - \sum_{p=0}^{m_0-1}\frac{2}{p!\,\Gamma(m_n)}\left(\frac{T_c}{\Omega_0\Omega_n}\right)^{\frac{p+m_n}{2}} K_{m_n-p}\left(\sqrt{\frac{4T_c}{\Omega_0\Omega_n}}\right)\right]\left(1 - e^{-\frac{x_0}{\Omega_I}}\right). \quad (A.7)$$

For I_2, use the change of variables $y = T_p(x)$ to obtain:

$$I_2 = \varphi_I e^{\frac{1}{\varpi\rho_S\Omega_I}}\left[\frac{e^{-\varphi_I T_c}}{\varphi_I} - \sum_{p=0}^{m_0-1}\frac{2}{p!\,\Gamma(m_n)}\left(\frac{1}{\Omega_0\Omega_n}\right)^{\frac{p+m_n}{2}} I_3\right], \quad (A.8)$$

where $\varphi_I = \frac{1}{\varpi\rho_S\tilde{\gamma}_{th}^{p,n}\Omega_I}$ and $I_3 = \int_{T_c}^\infty y^{\frac{p+m_n}{2}} K_{m_n-p}\left(\sqrt{\frac{4y}{\Omega_0\Omega_n}}\right)e^{-\varphi_I y}dy$.

Let $t = \frac{4}{\pi}\arctan(y - T_c) - 1 \Rightarrow y = \tan\left((t+1)\frac{\pi}{4}\right) + T_c \Rightarrow dy = \frac{\pi}{4}\sec^2\left((t+1)\frac{\pi}{4}\right)$, I_3 is given as:

$$I_3 = \frac{\pi}{4}\int_{-1}^{1}\sec^2\left(\frac{\pi(t+1)}{4}\right)\Delta(t)^{\frac{p+m_n}{2}} K_{m_n-p}\left(\sqrt{\frac{4\Delta(t)}{\Omega_0\Omega_n}}\right)e^{-\varphi_I\Delta(t)}dt, \quad (A.9)$$

where $\Delta(t) = \tan\left(\frac{\pi(t+1)}{4}\right) + T_c$.

Unfortunately, finding a closed-form expression for (A.9) is a tough task, but an accurate approximation can be obtained for it. By using Gaussian-Chebyshev quadrature [[31], Eq. (25.4.38)], (A.9) can be achieved.

$$I_3 \approx \frac{\pi^2}{4Q}\sum_{q=1}^{Q}\sqrt{1-\xi_q^2}\sec^2\left(\frac{\pi(\xi_q+1)}{4}\right)\Delta(\xi_q)^{\frac{p+m_n}{2}}e^{-\varphi_I\Delta(\xi_q)}K_{m_n-p}\left(\sqrt{\frac{4\Delta(\xi_q)}{\Omega_0\Omega_n}}\right), \quad (A.10)$$

where $\xi_q = \cos\left(\frac{2q-1}{2Q}\pi\right)$ and Q is a complexity-accuracy tradeoff parameter. Substituting (A.10) into (A.8), I_2 can be obtained as:

$$I_2 \approx \varphi_I e^{\frac{1}{\varpi\rho_S\Omega_I}}\left[\frac{e^{-\varphi_I T_c}}{\varphi_I} - \sum_{p=0}^{m_0-1}\sum_{q=1}^{Q}\frac{2\pi^2\sqrt{1-\xi_q^2}}{p!4Q\Gamma(m_n)}\left(\frac{1}{\Omega_0\Omega_n}\right)^{\frac{p+m_n}{2}}\sec^2\left(\frac{\pi(\xi_q+1)}{4}\right)\times\Delta(\xi_q)^{\frac{p+m_n}{2}}e^{-\varphi_I\Delta(\xi_q)}K_{m_n-p}\left(\sqrt{\frac{4\Delta(\xi_q)}{\Omega_0\Omega_n}}\right)\right] \quad (A.11)$$

Substituting (A.11) and (A.7) into (A.6) and applying the integration by parts, $\mathcal{P}_{U_n}^{\text{ipSIC}}$ can be re-expressed as:

$$\mathcal{P}_{U_n}^{\text{ipSIC}} \approx \left[1 - \sum_{p=0}^{m_0-1}\frac{2}{p!\,\Gamma(m_n)}\left(\frac{T_c}{\Omega_0\Omega_n}\right)^{\frac{p+m_n}{2}}K_{m_n-p}\left(\sqrt{\frac{4T_c}{\Omega_0\Omega_n}}\right)\right]\left(1-e^{-\frac{x_0}{\Omega_I}}\right)$$

$$+e^{\frac{1}{\varpi\rho_S\Omega_I}}\left[e^{-\varphi_I T_c} - \sum_{p=0}^{m_0-1}\sum_{q=1}^{Q}\frac{2\pi^2\varphi_I\sqrt{1-\xi_q^2}}{p!4Q\Gamma(m_n)}\left(\frac{1}{\Omega_0\Omega_n}\right)^{\frac{p+m_n}{2}}\sec^2\left(\frac{\pi(\xi_q+1)}{4}\right)\times\Delta(\xi_q)^{\frac{p+m_n}{2}}e^{-\varphi_I\Delta(\xi_q)}K_{m_n-p}\left(\sqrt{\frac{4\Delta(\xi_q)}{\Omega_0\Omega_n}}\right)\right]. \quad (A.12)$$

This completes the proof.

REFERENCES

[1] W. Jaafar et al., "On the Downlink Performance of RSMA-based UAV Communications," IEEE Trans. on Vehicular Technology, vol. 69, no. 12, pp. 16258-16263, 2020.

[2] F. Xiao et al., "Outage Performance Analysis of RSMA-aided Semi-grant-free Transmission Systems," IEEE Open J. of the Communications Society, vol. 4, pp. 253-268, 2023.

[3] T.-H. Vu et al., "On Performance of Downlink THz-based Rate-splitting Multiple-access (RSMA): Is It Always Better Than NOMA?," IEEE Trans. on Vehicular Techn., vol. 73, no. 3, pp. 4435-4440, 2024.

[4] P. Almers, f. Tufvesson and A. F. Molisch, "Keyhole Effect in MIMO Wireless Channels: Measurements and Theory," IEEE Trans. on Wireless Comm., vol. 5, no. 12, pp. 3596-3604, 2006.

[5] H. Zhang et al., "Performance Analysis of MIMO-HARQ Assisted V2V Communications with Keyhole Effect," IEEE Trans. on Comm., vol. 70, no. 5, pp. 3034-3046, May 2022.

[6] X. Zang et al., "On the Secrecy Performance of MIMOME Keyhole Channels Aided with Artificial Noise," IEICE Trans. on Comm., vol. E108-B, no. 5, pp. 631-639, May 2025.

[7] A. Krishnamoorthy and R. Schober, "Downlink MIMO-RSMA with Successive Null-space Precoding," IEEE Trans. on Wireless Communications, vol. 21, no. 11, pp. 9170-9185, 2022.

[8] O. Dizdar et al., "RSMA for Overloaded MIMO Networks: Low Complexity Design for Max-min Fairness," IEEE Trans. on Wireless Comm., vol. 23, no. 6, pp. 6156-6173, Jun. 2024.

[9] Y. Zhang et al., "Enhancing Secrecy in Hardware Impaired Cell-free Massive MIMO by RSMA," IEEE Trans. on Wireless Comm., vol. 23, no. 12, pp. 18788-18805, Dec. 2024.

[10] Y. Xu, Y. Mao, O. Dizdar and B. Clerckx, "Rate-Splitting Multiple Access With Finite Block Length for Short-packet and Low-latency Downlink Communications," IEEE Trans. on Vehicular Technology, vol. 71, no. 11, pp. 12333-12337, Nov. 2022.

[11] M. Katwe, K. Singh, B. Clerckx and C.-P. Li, "Rate Splitting Multiple Access for Energy Efficient RIS-aided Multi-user Short-packet Communications," Proc. of IEEE Global Communications Conf. (GLOBECOM) Workshops, pp. 644-649, Rio de Janeiro, Brazil, 2022.

[12] S. K. Singh, K. Agrawal, K. Singh, B. Clerckx and C.-P. Li, "RSMA Enhanced RIS-FD-UAV Aided Short Packet Communications under Imperfect SIC," Proc. of IEEE Global Communications Conf. (GLOBECOM) Workshops, pp. 1549-1554, Rio de Janeiro, Brazil, 2022.

[13] T.-H. Vu et al., "Rate-splitting Multiple Access-assisted THz-based Short-packet Communications," IEEE Wireless Communications Letters, vol. 12, no. 12, pp. 2218-2222, Dec. 2023.

[14] H. Shin and J. H. Lee, "Performance Analysis of Space-time Block Codes over Keyhole Nakagamim Fading Channels," IEEE Transactions on Vehicular Technology, vol. 53, no. 2, pp. 351-362, 2004.

[15] N. H. Tran, H. H. Nguyen and T. Le-Ngoc, "Performance Analysis and Design Criteria of BICMID with Signal Space Diversity for Keyhole Nakagami-m Fading Channels," IEEE Trans. on Information Theory, vol. 55, no. 4, pp. 1592-1602, Apr. 2009.

[16] C. Zhong et al., "Ergodic Mutual Information Analysis for Multi Keyhole MIMO Channels," IEEE Trans. on Wireless Communications, vol. 10, no. 6, pp. 1754-1763, Jun. 2011.

[17] L. K. S. Jayasinghe, N. Rajatheva, P. Dharmawansa and M. Latva-Aho, "Non-coherent Amplify-and Forward MIMO Relaying with OSTBC Over Rayleigh-Rician Fading Channels," IEEE Trans. on Vehicular Technology, vol. 62, no. 4, pp. 1610-1622, May 2013.

[18] A. M. Magableh et al., "Performance of Non-orthogonal Multiple Access (NOMA) Systems over N-Nakagami-m Multipath Fading Channels for 5G and Beyond," IEEE Trans. on Vehicular Techn., vol. 71,

no. 11, pp. 11615-11623, Nov. 2022.
[19] B. Ji et al., "Research on Secure Transmission Performance of Electric Vehicles under Nakagami-m Channel," IEEE Trans. on Intelligent Transportation Systems, vol. 22, no. 3, pp. 1881-1891, 2021.
[20] Z. Yang et al., "Optimization of Rate Allocation and Power Control for Rate Splitting Multiple Access (RSMA)," IEEE Transactions on Communications, vol. 69, no. 9, pp. 5988-6002, Sep. 2021.
[21] A. Krishnamoorthy and R. Schober, "Downlink Massive MU-MIMO with Successively-regularized Zero Forcing Precoding," IEEE Wireless Communications Letters, vol. 12, no. 1, pp. 114-118, 2023.
[22] X. Yue and Y. Liu, "Performance Analysis of Intelligent Reflecting Surface Assisted NOMA Networks," IEEE Trans. on Wireless Communications, vol. 21, no. 4, pp. 2623-2636, Apr. 2022.
[23] D.-T. Do et al., "UAV Relaying Enabled NOMA Network With Hybrid Duplexing and Multiple Antennas," IEEE Access, vol. 8, pp. 186993-187007, 2020.
[24] D.-T. Do et al., "Antenna Selection and Device Grouping for Spectrum-efficient UAV-Assisted IoT Systems," IEEE Internet of Things Journal, vol. 10, no. 9, pp. 8014-8030, May 2023.
[25] M. Elsayed et al., "Symbiotic Ambient Backscatter IoT Transmission Over NOMA-enabled Network," Proc. of IEEE Int. Conf. on Communi. (ICC), pp. 1549-1554, Seoul, S. Korea, 2022.
[26] I. S. Gradshteyn and I. M. Ryzhik, Table of Integrals, Series and Products, ISBN-10: 0-12-373637-4, Academic Press, 2014.
[27] T.-T. T. Dao, S. Q. Nguyen, H. N. Nguyen, P. X. Nguyen and Y.-H. Kim, "Performance Evaluation of Downlink Multiple Users NOMA-Enable UAV-aided Communication Systems Over Nakagami-m Fading Environments," IEEE Access, vol. 9, pp. 151641-151653, 2021.
[28] X. Yue, Y. Liu, S. Kang, A. Nallanathan and Z. Ding, "Exploiting Full/Half-duplex User Relaying in NOMA Systems," IEEE Trans. on Communications, vol. 66, no. 2, pp. 560-575, Feb. 2018.
[29] N. Jaiswal and N. Purohit, "Performance Analysis of NOMA-enabled Vehicular Communication Systems with Transmit Antenna Selection over Double Nakagami-m Fading," IEEE Trans. on Vehicular Technology, vol. 70, no. 12, pp. 12725-12741, Dec. 2021.
[30] Y. Cheng, K. H. Li, Y. Liu, K. C. Teh and H. V. Poor, "Downlink and Uplink Intelligent Reflecting Surface Aided Networks: NOMA and OMA," IEEE Trans. on Wireless Communications, vol. 20, no. 6, pp. 3988-4000, Jun. 2021.
[31] M. Abramowitz and I. A. Stegun, Handbook of Mathematical Functions with Formulas, Graphs and Mathematical Tables, vol. 55, US Government Printing Office, 1948.

ملخص البحث:

تتناول هذه الورقة البحثية الأداء النّظري لتقنية الوصول المتعدّد بتقسيم المعدّل (RSMA) في قنوات التّلاشي ذات التّقْب المفتاحي. وتُعرف هذه البيئة ذات الرُّتبة المنخفضة بتأثيرها السلبي على أداء أنظمة الإدخال والإخراج الأحادي التّقليدية (SISO). وقد تمّ اشتقاق نتائج دقيقة وتقريبية لاحتمالية انقطاع الخدمة لتقنية (RSMA) بالنّسبة لقناة وصلة هابطة ثنائية المستخدمين، مع إلغاء التّداخُل المتتالي الكامل وغير الكامل. ويتمّ استخلاص الحلول المغلقة من خلال مقارنة حاصل ضرْب قناتَي تلاشٍ مستقلّتين تُحاكيان تأثير تقْب المفتاح. ولإثبات متانة تقنية الوصول المتعدّد بتقسيم المعدّل في مثل هذه البيئة، ندْرس أيضاً رتبة التّنوُّع ونكشف تأثير نقْص الرُّتبة النّاتج عن ثقْب المفتاح على موثوقية النّظام. وتُظهر نتائجنا أن التّقنية المذكورة تحتفظ بميزة أداء على الوصول المتعدّد غير المتعامد، خاصّةً مع عدم مثالية إلغاء التّداخل الثنائي أو انخفاض نسبة الإشارة إلى الضّجيج. وتؤكّد النّتائج العدّدية ومحاكاة مونت كارلو الصِّيغ النظرية، وتُبين أنّ تقنية الوصول المتعدّد بتقسيم المعدّل يمكنها مكافحة الآثار الضّارّة لقناة ثقْب المفتاح بشكلٍ أفضل من المخطّطات التّقليدية الأخرى. كذلك تؤكّد النّتائج امكانات تلك التّقنية لأنظمة الاتّصالات اللاسلكية المستقبلية الّتي تعمل في بيئات تلاشٍ شديد.